Supplementary Information

Two fluorinases prioritized from protein families of fluorinase, SAM-dependent chlorinase and hydroxide adenosyltransferase

Kai He,[a] Yue Yan,[a,b] Shuting Feng,[a] Pinmei Wang,[a] Zhizhen Zhang[a] and Nan Wang[*a]

[a] *Ocean College, Zhejiang University, 1 Zheda Rd., Zhoushan 316021, China. E-mail: n_wang@zju.edu.cn.*

[b] *School of Traditional Chinese Medicines, Shenyang Pharmaceutical University, 103 Wenhua Rd., Shenyang 110016, China*

** Corresponding author*

Content

1. Materials and Methods

1.1 Bioinformatic Analysis

The EFI-EST web tool (https://efi.igb.illinois.edu)[1, 2] was used for fluorinase (FIA) discovery from public protein databases. Totally 13,857 proteins were retrieved from the Pfam and InterPro Families of IPR030978 (Fluorinases), IPR002747 (SAM hydroxide adenosyltransferases) and PF20257 (SAM hydroxide adenosyltransferase C-terminal domain, also known as DUF62). After remove the fragments and incomplete sequences, 12,718 proteins were used to generate SNN with an e-value of 5 (negative log) for BLAST to calculate edge alignment score similarities. The resulting SNN was visualized by Cytoscape[3] showing sequence identities in the range of 53~100%. The known FIAs were used as indicators of FIA clustering.

The protein sequences were aligned using Clustal Omega[4] and the phylogenetic tree was generated using the JTT method and the maximum likelihood algorithm using MEGA 11.0.14.[5] AlphaFold2[6] was used for structure predictions of the proteins described in the main context.

1.2 Strains, plasmids and reagents

Strains, plasmids, PCR primers used in this study are listed in Tables S2–S5, respectively. *Escherichia coli* DH5α was used for general cloning and subcloning. *E. coli* BL21 was used for protein production. They were maintained and used as described elsewhere.[7] SAM (*S*-adenosyl-L-methionine, 98%) were purchased from Chentong Biochem (Hangzhou, China). 5′-FDA (98%) were obtained from Haohong Biotech (Hangzhou, China). Primers used in this study (Table S4) were synthesized by Sunya (Hangzhou, China). Enzymes and buffers for molecular cloning were purchased from TransGen Biotech, TAKARA and NEB and were used by following the protocols provided by the manufacturer. DNA gel extraction and plasmid preparation kits were purchased from Sangon (Shanghai, China). DNA sequencing was conducted by Sunya (Hangzhou, China). Antibiotics, other chemicals and medium components were purchased from regular commercial sources, including Sinopharm (Beijing, China), Oxoid (Beijing, China), and Macklin (Shanghai, China).

1.3 Gene cloning

Codon optimized DNA sequences encoding the hypothetic FIAs and the known fluorinase FIA$^{Sxin\ 8}$ (Table S5) were synthesized and cloned in-frame into the NdeI/XhoI cloning site of the pET28a(+) (Novagen, Madison, WI) to afford plasmids for protein production. Gene expression is controlled by the T7 promoter on the backbones of the constructs. All the proteins are 6 His-tagged at the C-termini to facilitate purification *via* Ni-NTA affinity chromatography. All the constructs were verified by colony PCR, restriction digests and sequencing of the plasmids. Constructs with correct inserts were used to transform the competed cells of *E. coli* BL21(DE3). The resulting transformants were used for heterologous protein production.

1.4 Protein production and purification

The protein production strains constructed with *E. coli* BL21 were cultured in 500 mL of lysogeny broth (LB) medium containing 50 μg/mL kanamycin at 37 °C with shaking at 250 rpm. Gene expression was induced with 0.6 mM isopropyl β-D-1-thiogalactopyranoside (IPTG) at OD_{600} of 0.6~0.8, and then continue the fermentation at 16 °C for 12 h. The fermentation broths were then centrifuged at 4000 rpm 4 °C for 20 min. The cell pellets were collected and suspended into 50 mM Tris buffer (pH 8.0) containing 300 mM NaCl and 10% glycerol. Cell lysis was performed using a combination of lysozyme digestion and ultrasonication. The resulting mixtures were centrifugated for 30 min at 15000 rpm at 4°C to afford supernatants ready for protein purification with an ÄKTA FPLC system (GE, USA) equipped with a 5-mL HisTrap^{TM} HP column (GE Healthcare Bio-Science AB). The column was eluted stepwise with mixtures of the binding buffer and the elution buffer. Both the binding buffer (A), containing 20 mM imidazole, and the elution buffer (B), containing 500 mM imidazole, were prepared using 100 mM Tris buffer (pH 8.0) with 300 mM NaCl. Wash the column with 6% B in A (v/v) to remove the nonspecific proteins. Pure proteins were eluted at 57% B in A (~300 mM imidazole). The eluents containing pure proteins were collected and concentrated to ~1 mL with Amicon Ultra-15 (Merck Millipore) centrifugal ultrafilters. The proteins were reconstituted in 10 mL 50 mM phosphate buffer (pH 7.4) and repeated the ultrafiltration 3 times to remove the salt. Concentrations of the purified proteins were determined by bicinchoninic acid (BCA) protein assay kit (Beyotime, Shanghai,

China).[9] Aliquots of each protein were frozen in liquid nitrogen and stored at -80 °C until use.

1.5 HPLC and LC-TOFMS analysis

HPLC analyses were performed on a SHIMADZU LC-20 equipped with a DAD detector and a YMC-Triart C18 column (4.6 mm × 250 mm, 5 μm). The production of 5′-FDA was detected and determined at 254 nm. The column with a constant temperature of 35 °C was eluted gradiently with aqueous methanol at a flowrate of 0.6 mL/min. The elution gradients are 0–5 min, 5–20% methanol; 5–15 min, 20–30% methanol; 15–20 min, 30–90% methanol; 20–30 min, 100% methanol. LC-TOFMS analyses for enzymatic product identification were performed on an Agilent 1260 Infinity LC module coupled to a UV detector and a 6230 ESI-TOF mass spectrometer. LC-TOFMS was run in positive mode using the same HPLC column and elution gradients.

1.6 Fluorination activity assay

Fluorination activity of the enzymes was assayed in 50 mM phosphate buffer, pH 7.4. Each 500-μL reaction mixture contains 3 μM (hypothetic) FIA, 100 mM KF and 1 mM SAM. The enzymes were preincubated with KF for 5 min at 37 °C, followed by the addition of SAM to initiate the reaction. After incubation at 37 °C for 30 min, 500 μL of methanol was added to each reaction mixture to quench the reaction. The reaction mixtures were then centrifuged at 15,000 rpm for 20 min at 4 °C and the supernatant was then analyzed by LC-TOFMS and analytical HPLC with UV detection at 254 nm. Production of 5′-fluoro-5′-deoxyadenosine (5′-FDA) indicates fluorinating activity. The reactions conducted with boiled enzymes were used as negative controls.

1.7 *In vitro* enzymatic assays for chlorinase and SAM hydroxide adenosyltransferase activities

For the chlorination reaction, all enzymes were assayed in 50 mM phosphate buffer (pH 7.4), following conditions similar to those in Section 1.5. Each 500-μL reaction mixture contained 3 μM hypothetical FIA, 1 mM SAM, and 100 mM NaCl. Enzymes were pre-incubated with NaCl for 5 minutes at 37 °C, and the reaction was initiated by adding SAM. After 30 minutes of incubation at 37 °C, each reaction was quenched by adding 500 μL of

methanol. For the hydroxylation reaction, NaCl was replaced with water under otherwise identical conditions. The reaction mixtures were centrifuged at 15,000 rpm for 20 minutes at 4 °C, and the resulting supernatants were analyzed by LC-TOFMS and analytical HPLC with UV detection at 254 nm. The production of 5′-chloro-5′-deoxyadenosine (5′-ClDA) or adenine indicated chlorinating or hydroxylating activity, respectively. Reactions performed with heat-inactivated enzymes served as negative controls.

1.8 Standard curve of 5′-FDA

The 5 mM stock solution of 5′-FDA was used to prepare the calibration working solutions by serial dilution with deionized water to concentrations in the range of 1~1000 μM. Each working solution was prepared in triplicate and tested by HPLC. The calibration curve for 5′-FDA was constructed by plotting peak areas versus concentrations. The correlation coefficient (R^2) between peak area and the concentration was calculated.

1.9 Influence of temperature, pH and metals on the fluorination activity

To determine the optimums of temperature, pH and metal dependence for the purified enzymes, their relative fluorination activity was measured at temperatures ranging from 20 to 70 °C, and at pH values from 4.0 to 11.0. Buffer systems used were 200 mM acetate sodium (pH 4.0–5.0), 200 mM sodium phosphate (pH 5.0–8.0); 50 mM Tris–HCl (pH 7.0–9.0); 50 mM glycine–NaOH (pH 9.0–10.0) and Na_2CO_3-NaOH (pH 10.0–11.0). Enzyme was added to different buffers to a final concentration of 3 μM and allowed to sit for 5 min at 37 °C. Reactions were initiated by adding substrates KF (100 mM) and SAM (1 mM). After 30 minutes, each reaction mixture (500 μL) received 500 μL methanol to quench the reaction. The resulting mixtures were centrifuged at 15,000 rpm for 20 min, and the production of 5′-FDA in the supernatants was analyzed by HPLC. Eight divalent metal ions (10 mM) were tested for their effects on the enzymatic activity of FIA^{Sbac}, including Mn^{2+}, Fe^{2+}, Co^{2+}, Cu^{2+}, Ca^{2+}, Zn^{2+}, Mg^{2+} and Ni^{2+}. The metal dependence of FIA^{Sbac} was assessed using 10 mM EDTA.

1.10 Kinetics studies of FIA^{Sbac}

Working solutions of SAM were prepared in triplicates with concentrations in the range of

10–400 μM. The enzymatic reaction for kinetic assays were performed in 300 μL phosphate buffer (50 mM, pH 7.4) containing 100 mM KF at 37 °C. Each kinetic assay was performed in triplicate. Reaction was started by adding enzyme (3 μM) and different concentrations of SAM. A portion of 50 μL sample was collected from each reaction mixture at 1, 3, 5, 7 and 10 min, and immediately quenched with equal volume of methanol. The resulting solutions were centrifuged at 13000 rpm for 10 min to afford the supernatant for HPLC analysis of the 5′-FDA production. The 5′-FDA formed at different reaction times were determined using the calibration curve mentioned earlier. Plotting the concentration 5′-FDA against reaction times at each SAM concentration allowed for the determination of the initial reaction rate of 5′-FDA at different SAM concentrations. GraphPad Prism 9 was then utilized to fit the Michaelis-Menten curve and calculate the enzymatic kinetic constants of the substrate SAM.

2. Supplementary Tables

Table S1 The seven hypothetical fluorinases

The seven hypothetical fluorinases clustered with known FIAs in the SNN generated by EFI-EST.

Name	Organism	UniProt ID
FIA^{Sbac}	*Streptosporangiales* sp.	A0A7J9ZI22
FIA^{Cbac}	*Chloroflexi* sp.	A0A535N3L3
FIA^{Adig}	*Actinoplanes digitatis*	A0A7W7MQB5
FIA^{Smor}	*Streptomyces morookaense*	A0A7Y7B3E7
FIA^{Tnor}	*Thermodesulforhabdus norvegica*	A0A1I4QPY6
FIA^{Pbac}	*Peptococcaceae* sp. CEB3	A0A0J1FI89
FIA^{Gbac}	*Geodermatophilaceae* sp.	A0A7W0NIE1

Table S2 Strains used in this study

Strains used in this study

Strain	**Description**
E. coli BL21(DE3)	Protein production
E. coli DH5α	Molecular cloning
E. coli TOP10	Molecular cloning
E. coli BL_*FlASbac*	Protein production of FlA^{Sbac}
E. coli BL_*FlACbac*	Protein production of FlA^{Cbac}
E. coli BL_*FlAAdig*	Protein production of FlA^{Adig}
E. coli BL_*FlASmor*	Protein production of FlA^{Smor}
E. coli BL_*FlATnor*	Protein production of FlA^{Tnor}
E. coli BL_*FlAPbac*	Protein production of FlA^{Pbac}
E. coli BL_*FlAGbac*	Protein production of FlA^{Gbac}

Table S3 plasmids constructed in this study

Plasmids constructed in this study.

Plasmid	**Description**
pET-28_ *FlASbac*	Gene expression for the production of FlA^{Sbac}
pET-28_ *FlACbac*	Gene expression for the production of FlA^{Cbac}
pET-28_ *FlAAdig*	Gene expression for the production of FlA^{Adig}
pET-28_ *FlASmor*	Gene expression for the production of FlA^{Smor}
pET-28_ *FlATnor*	Gene expression for the production of FlA^{Tnor}
pET-28_ *FlAPbac*	Gene expression for the production of FlA^{Pbac}
pET-28_ *FlAGbac*	Gene expression for the production of FlA^{Gbac}

Table S4 PCR primers used in this study

PCR primers used in this study

Name	**Function**	**Sequence (5′ to 3′)**
T7-F	Colony PCR	TAATACGACTCACTATAGGG
T7-R	Colony PCR	TGCTAGTTATTGCTCAGCGG
Sxin-W50F-F	Site-directed mutagenesis	CCACAGCATGACCCCGTTTGATGTGGAGGAAGGTG
Sxin-W50F-R	Site-directed mutagenesis	CACCTTCCTCCACATCAAACGGGGTCATGCTGTGG
Sbac-F50W-F	Site-directed mutagenesis	CATACCATGACCCCGTGGGATGTGGTGGAAGG
Sbac-F50W-R	Site-directed mutagenesis	CCTTCCACCACATCCCACGGGGTCATGGTATG
Sxin-W50A-F	Site-directed mutagenesis	CCACAGCATGACCCCGGCGGATGTGGAGGAAGGTG
Sxin-W50A-R	Site-directed mutagenesis	CACCTTCCTCCACATCCGCCGGGGTCATGCTGTGG
Sbac-F50A-F	Site-directed mutagenesis	CATACCATGACCCCGGCTGATGTGGTGGAAGG
Sbac-F50A-R	Site-directed mutagenesis	CCTTCCACCACATCAGCCGGGGTCATGGTATG
flA-tag	Stop-codon replacement	GTGCTCGAGTGCGTTGGTCTCAACACGCACTTTCA

Table S5 The amino acid sequences of the seven hypothetic fluorinases and FIA*Sxin*

The amino acid sequences of the seven hypothetic fluorinases and FIA*Sxin*

Name	Amino acid sequence
FIA*Sbac*	MTANGSRRPTIAFMSDLGVTDDSVAQCKGLMLSICPDVNIIDICHTMTPFDVVEGARYI VDLPRYFPEGTVFATTTYPATGTTARSVAIRLKRAALGGARGQLAGSGKGFERAEGA YIYIAPNNGLLTRVIEEHGYLEAYEVSSTDVIPERPEPTFYSREMVAIPSAHLAAGFPLE KVGRKLEDHEIVRFEQKKGAVAGEALVGEVSAIDHPFGNVWTNLHRTDLEKAGIKYGT PMKIVVDGVLPFELPLSPTFADAEGPGAPVAYLNSRGYLSVARNAASLAYPYNLNAGM SVRVTTA
FIA*Gbac*	MSDLGTVDDSVGICKGLMLSICPDATIVDICHAMTPWDIKQGARLIVDLPRYYPEWTVF ATTTYPDTGTAMRSVAIRVPKGQVYVAPNNGLLTSVIEDHGFVEAYEVTSTEVIPEEPE PTFFSREMVAVPSAHLAAGFPLDQVGRPLKDEEIVRFENQHPVVVEDGALRGILTNVD WPYGNVWVNIRQSVLEANGIGYGTKVKITIDDVLPFELQLTRTFGDVPLGAPVTYLSSR GYLGIARNRANLADTYNLRQGMSVTVKAC
FIA*Adig*	MSDLGTTDDSVAQCKGLMLSICPSVTIVDVCHSMTPWDVVEGARYIVDLPRFFPEGTV FATTTYPATGTGTRSVALRIKQAALGGARGQWAGSGAGLERAEGSYIYIAPNNGLLTT VIEEHGYIEAYEVSNTKVIPAEPEPTFYSREMVAIPSAHLAAGFPLNEVGRQLSDDEIVR FERPKASTVSGGVLSGTITNVDHPFGNLWTNIHRTDLEKAGIGYQTQLKLVLDGVLTFD LPLVPTFADAGKIGDPVIYINSRGYLALARNAAPLAYPYNLKAGISVAVTKA
FIA*Smor*	MSDLGTTDDSVAQCKGLMHSICPGVTVVDVCHSMTPWDVEEGARYIVDLPRFFPEGT VFATTTYPATGTTTRSVAVRIRQAAKGGARGQWAGSGDGFERADGSYIYIAPNNGLLT TVLEEHGYIEAYEVTSTKVIPANPEPTFYSREMVAIPSAHLAAGFPLAEVGRRLDDSEIV RFHRPAVEISGDTLSGVVTAIDHPFGNIWTNIHRVDLEKAGIGHGKHLRIILDDVLPFEA PLTPTFADAGAIGNIAFYLNSRGYLSLARNAASLAYPYNLKAGLKVRVETR
FIA*Pbac*	MEKVDNKTVFQRPIIAFMSDLGAFDDSVGICKGLMLSVCPEAQIIDICHSMTPFDVEQG ARLIVDLPRFFPEGRTVFATTTYPATGTMARSLALRIKRPAKGGALGQWAGAGFGIER GVGGYIYVAPNNGLLTDVIEEHGYLEAYEITSTNVIPENPEPTFFSREMVALPSAYLAA GYPLSEVGQPLGDSEIVRFKKVLPRKMSESELVGVVAAIDRPFGNVWTNISRRDLDKI GVTYGSQLKVVLDNALMFELPLSQTFADAREIGAAVAYINSRGHLSLGRYAANLADRY NINRGMPIRLKVITG
FIA*Cbac*	MSDLGTFDDSVGICKGLMLSVCPDVVIVDICHAMTPFDIEEGARLIVDLPRFFPEGTVF ATTTYPATGTSTRSVALRIRQAAVGGARGQWAGAGEGIQRAEGAYIYIAPNNGLLTSVI EEHGYLEAYEVTSTSVIPARPEPTFFSREMVAVPAAHLAAGFPLSQVGRPLQDSEIVR FDRRRPASLGDGGFAGVITVVDRPYGNVWTNISRKDLANQGIAYGTRLRITVDNVLPF DLTLTPTFADAGEIGAPVCYVNSRGYLSLARNASNLADTYNIRRHMPVNVQVVSRTDG EPHRSESSELASVKGT
FIA*Tnor*	MDIGPIIGFASDLGLKDDSVALCKGLMISICPEVYIVDICHTMTPFDIEEGAWLALDLPRF FPEGRTIFAVTTYPATGTEARSIAVRIKKAVPGGSLEKWEGPGGGMERTLEGGYIYVA PNNGLLTFVLERYGYIEAYEIISTEFIPENPEPTFFSREMVAIRAACIAKKVVSQGVPLSK VGPPITEDKLARIKLSLPEKIAHNEIRGKIIRIDYPYGNVWTNISFNDLKSMGINYGSRLT VVIGDILSFNVYLTRTFADAGGIGDVISYINSRGYFSLGGYAANLADLCNLRRGMNVVVI KV
FIA*Sxin*	MSADPTQRPIIGFMSDLGTTDDSVAQCKGLMHSICPGVTVIDVCHSMTPWDVEEGAR YIVDLPRFFPEGTVFATTTYPATGTETRSVAVRIKQAAKGGARGQWAGSAGGFERAE GSYIYVAPNNGLLTTVLEEHGYIEAYEVSSTKVIPERPEPTFYSREMVAIPAAHLAAGFP LSEVGRPLEDSEIVRYQPPQVEISGDTLTGVVSAIDHPFGNVWTNIHRTHLEKAGIGYG KRIKIILDDVLPFEQTLVPTFADAGEIGGVAAYLNSRGYLSLARNAASLAYPFNLKAGLK VRVETN

3. Supplementary Figures

Fig. S1 Distribution of the 12718 proteins for SNN calculation using the EFI-EST online tool.

Distribution of the 12718 proteins for SNN calculation using the EFI-EST online tool. The proteins were retrieved from the Pfam/InterPro Families of IPR002747, PF20257 and IPR030978.

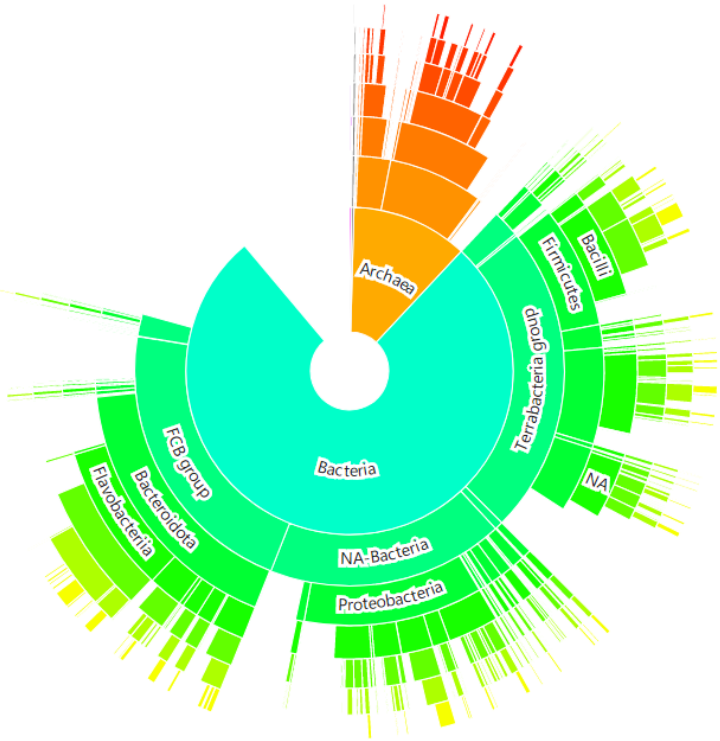

Fig. S2 Phylogenetic analysis

Maximum likelihood phylogenetic analysis with bootstrap values (1000 replicates) from the protein sequences of hypothetic fluorinases (black), fluorinase (red), a SAM-dependent chlorinase (green) and a SAM hydroxide adenosyltransferase (blue).

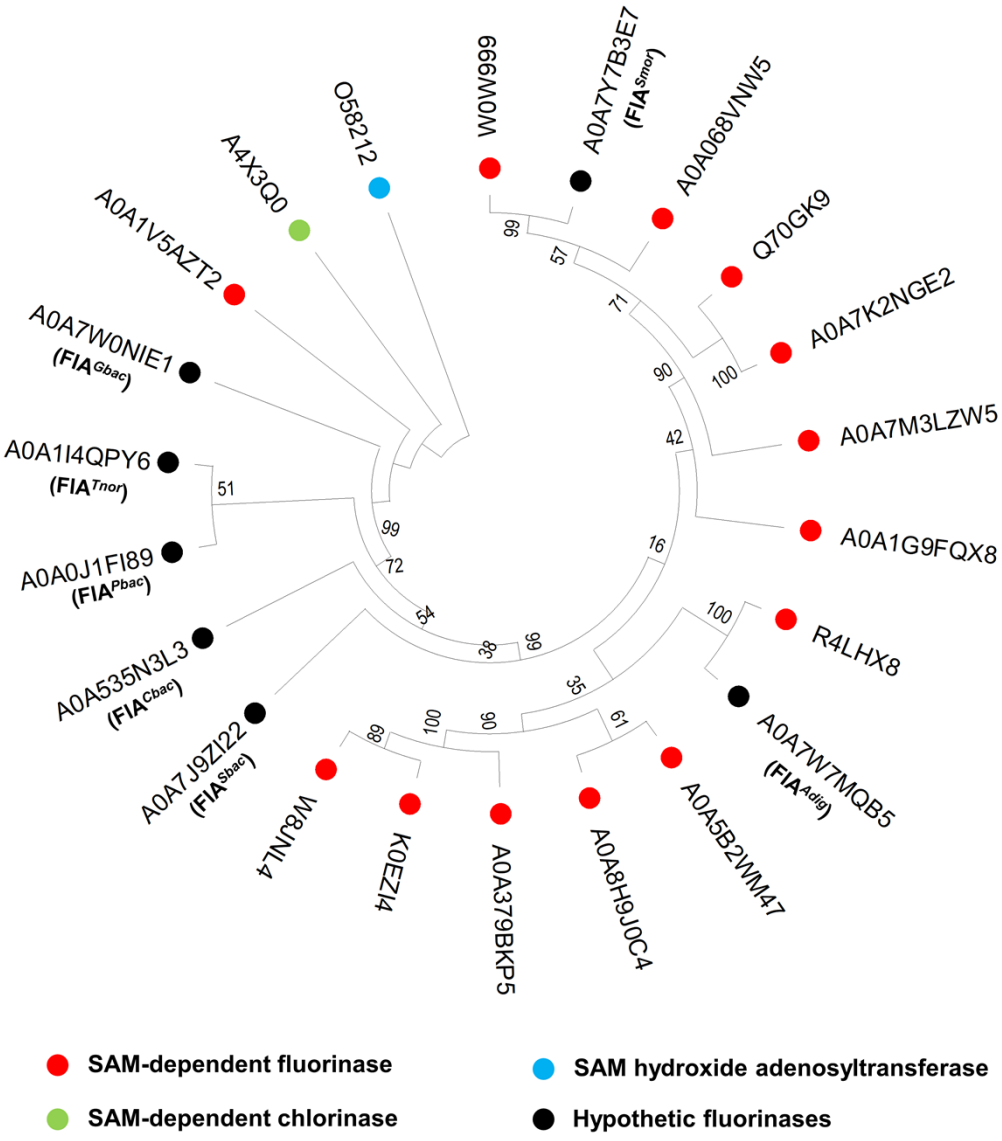

Fig. S3 SDS-PAGE analysis of the hypothetic fluorinases

SDS-PAGE analysis of the seven hypothetic fluorinases of and FIA^{Sxin} produced in *E. coli* BL21. A: Cell pellets; B: Supernatants; lane M: Marker; The black arrows indicate the bands of hypothetic fluorinases.

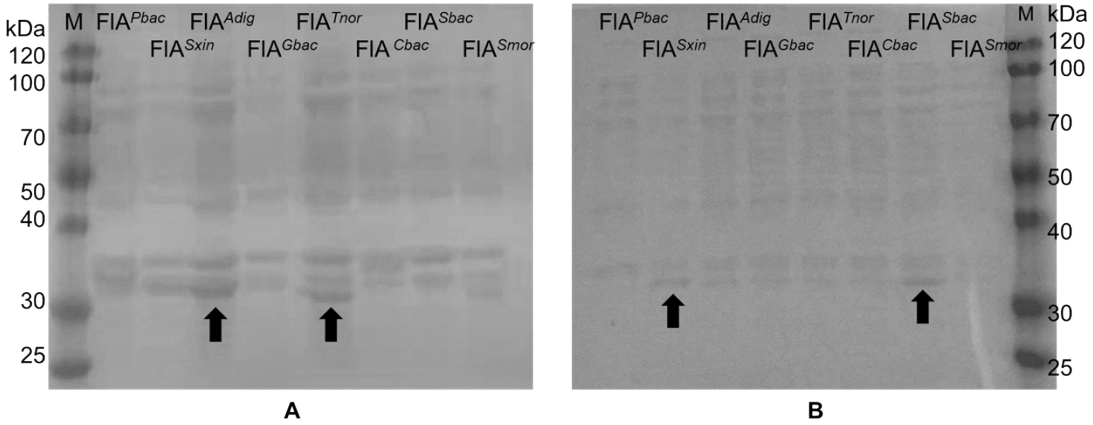

Fig. S4 SDS-PAGE analysis of the soluble fractions of the hypothetic fluorinases

SDS-PAGE analysis of the soluble fractions of the hypothetic fluorinases and FIA^{Sxin}

A: Soluble proteins purified from the supernatant fractions; B: Soluble proteins obtained via refolding of inclusion bodies; Lane 1: Eluent from wash buffer of FIA^{Adig}; Lane 2: Eluent from the wash buffer of FIA^{Tnor}; Lane 3: Eluent from wash buffer of FIA^{Smor}.

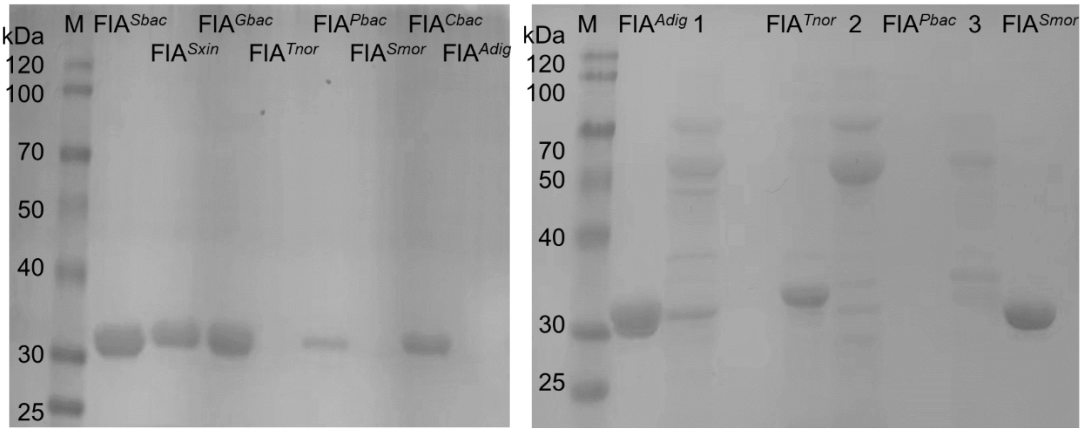

Fig. S5 The *in vitro* fluorination activity assays.

HPLC analysis of the fluorination activity of the seven hypothetic fluorinases using SAM and F^- as substrates. The retention times of 5′-FDA and adenosine are 18 min and 13 min, respectively.

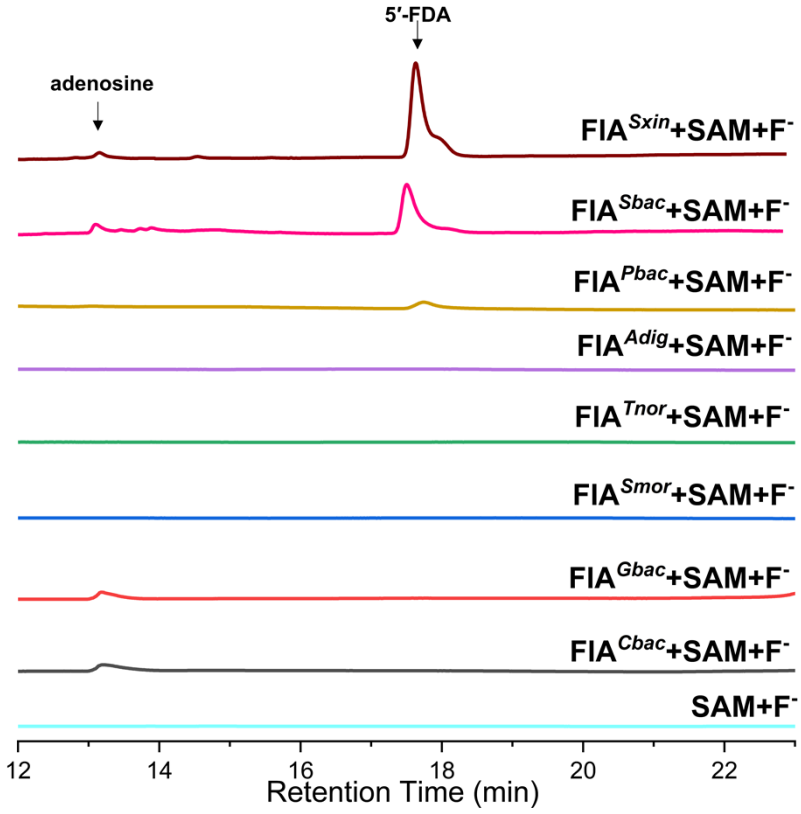

Fig S6 Chlorinase activity of FIA^{Sxin} and FIA^{Sbac}

EIC (Extracted ion chromatogram) from LC-TOFMS experiments showing the chlorination activity of FIA^{Sxin} (**a**) and FIA^{Sbac} (**b**) using SAM and Cl^- as substrates. Product 5′-ClDA was identified by the adduct ions at *m/z* 286.0701 and 286.0706, calculated for $[M+H]^+$ ($C_{10}H_{12}ClN_5O_3^+$) at *m/z* 286.0701. **c**: 5′-ClDA standard; **d**, 5′-ClDA detected in FIA^{Sxin} catalyzed reaction mixture; **e**, 5′-ClDA detected in FIA^{Sbac} catalyzed reaction mixture.

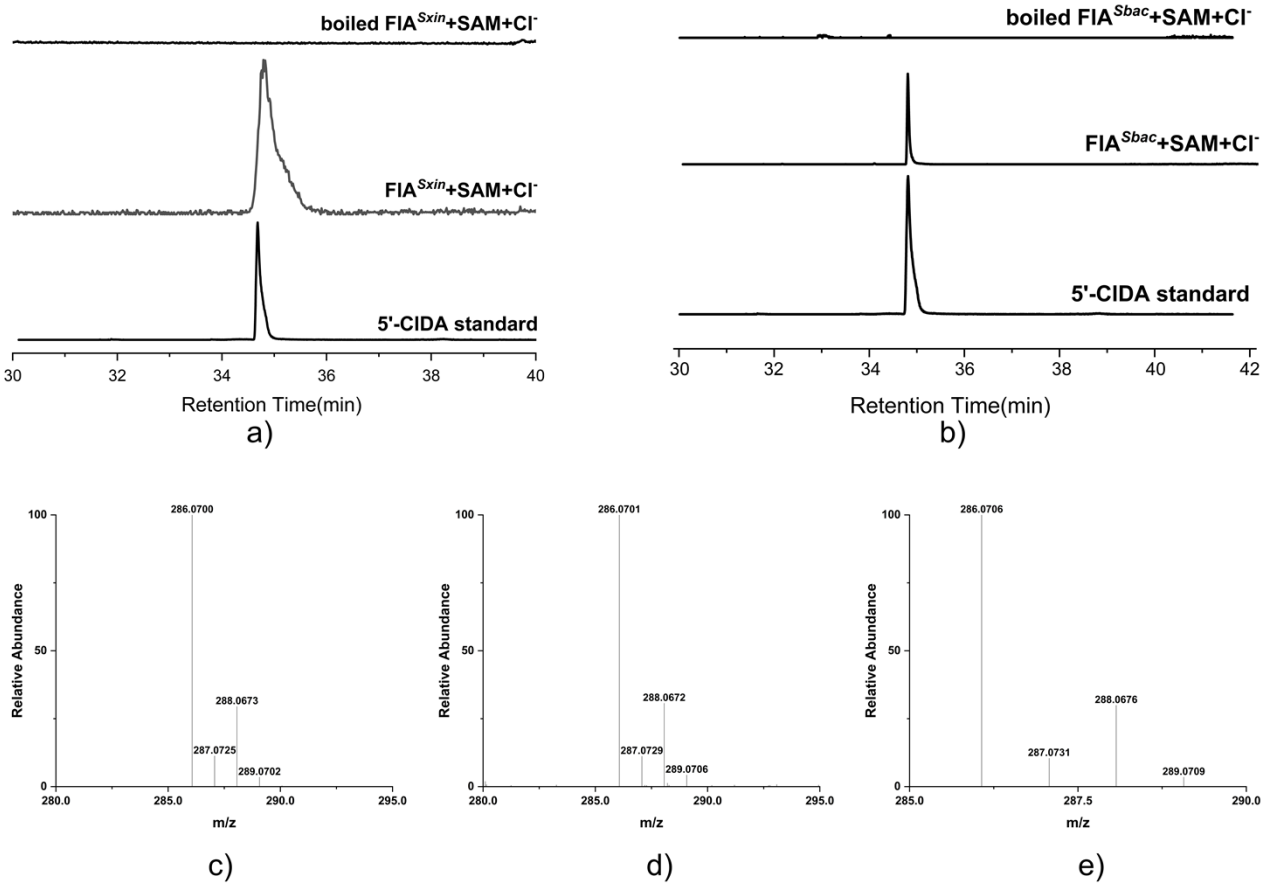

Fig. S7 Effect of temperature on the activity of FIA^{Sbac}

Effect of temperature on the activity of FIA^{Sbac}. The relative activity was calculated within the temperature range of 20–70 °C. The highest relative activity was observed at 50 °C.

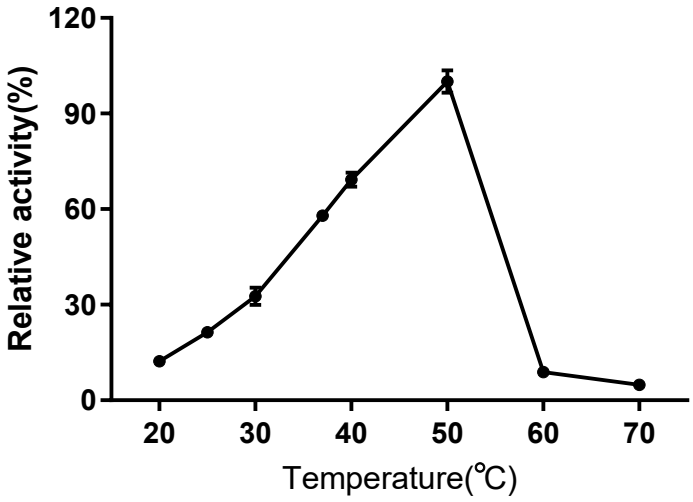

Fig. S8 Effect of pH on the activity of FlA^{Sbac}.

Effect of pH on the activity of FlA^{Sbac}. The relative activity was measured across the pH range of 5.0–10.0 using buffers including acetate, phosphate, tris-HCl, glycine-NaOH and Na_2CO_3-NaOH. The highest relative activity was observed in phosphate buffer at pH 7.0.

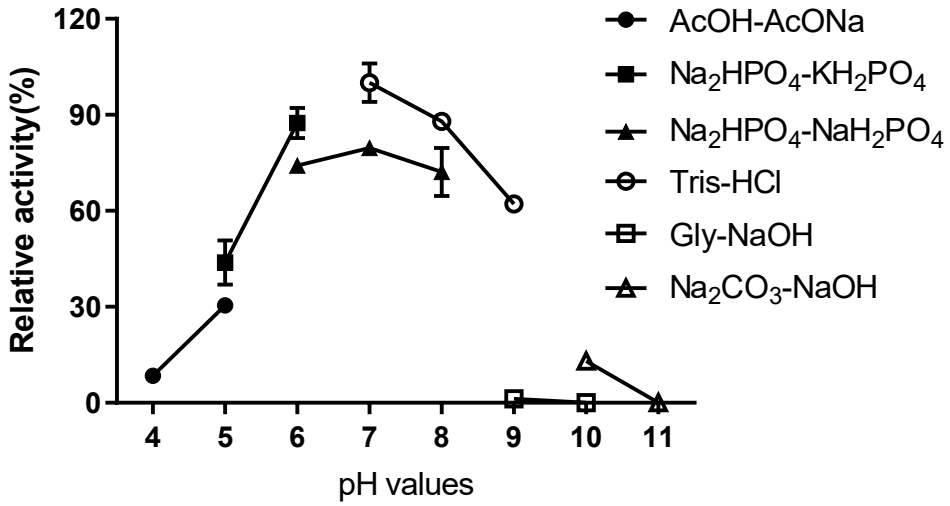

Fig. S9 The dependence of FIA^{Sbac} on divalent metal ions.

The divalent metal ion dependence of FIA^{Sbac}. Eight divalent metal ions (10 mM) were tested for their effects on the enzymatic activity of FIA^{Sbac}, including Mn^{2+}, Fe^{2+}, Co^{2+}, Cu^{2+}, Ca^{2+}, Zn^{2+}, Mg^{2+} and Ni^{2+}. The presence of Cu^{2+} resulted in nearly complete (>98%) abolishment of the fluorination activity of FIA^{Sbac}. Other metals caused activity loss less than 20%. Addition of 10 mM EDTA showed comparable relative activities supporting that FIA^{Sbac} does not require divalent metal ions for fluorination.

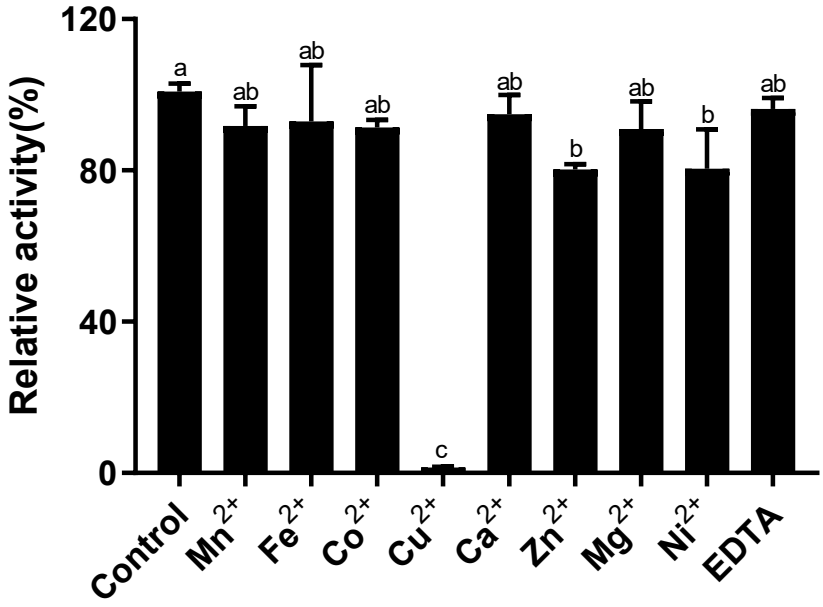

Fig. S10 The Michaelis-Menten curve for FIA^{Sxin}

The Michaelis-Menten curve for SAM in the FIA^{Sxin} catalyzed fluorination reactions. K_m = 27 ± 7 μM, k_{cat} = 0.37 ± 0.02 min^{-1}, V_{max} = 1.1 ± 0.1 μM min^{-1}, k_{cat}/K_m = 13.6 ± 0.8 mM^{-1} min^{-1}.

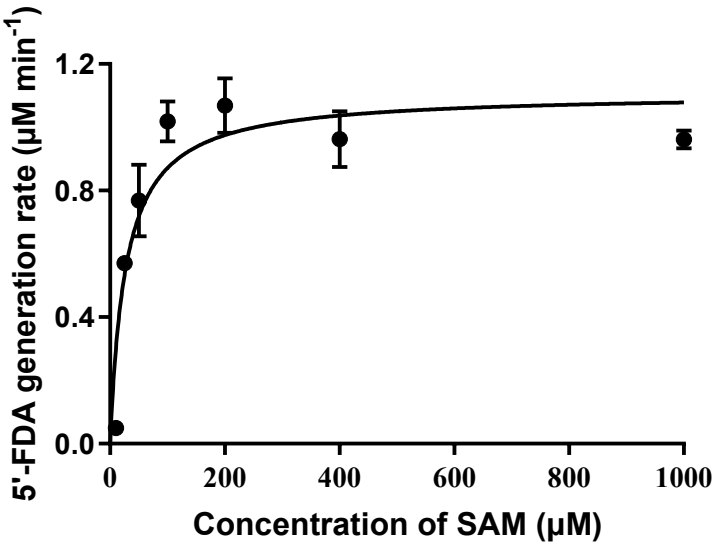

Fig. S11 Multiple sequence alignments

Multiple sequence alignments of the hypothetic fluorinases from SNN (black), known fluorinases (red), a chlorinase (green) and a hydroxide adenosyltransferase (blue). The sequence in the red box is the loop region unique to most fluorinases, and the key catalytic sites are marked with stars.

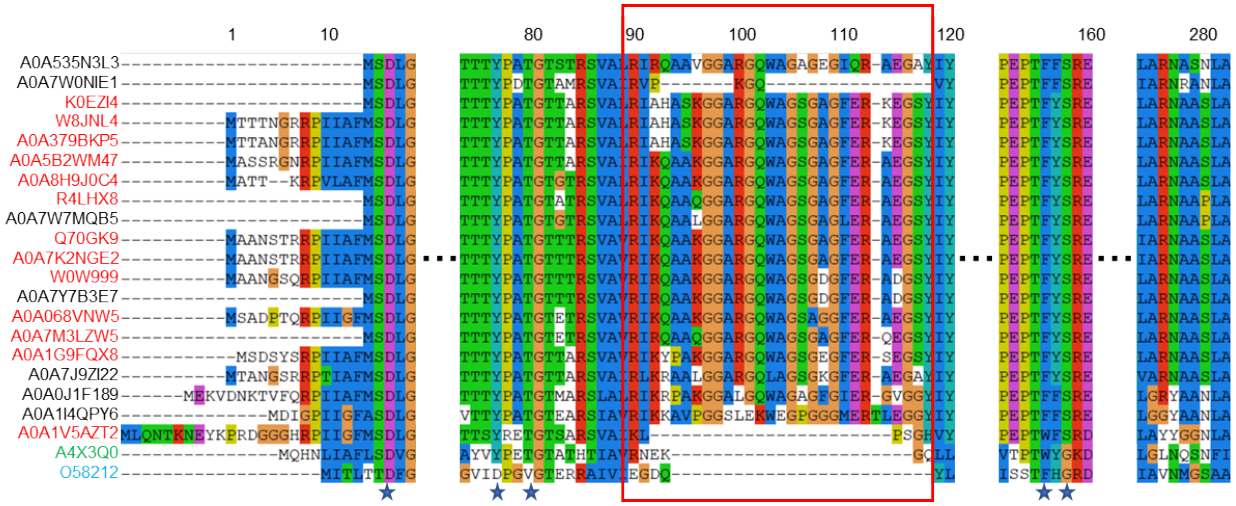

Fig. S12 Structural comparison of FIA^{Sbac} with FIA^{Scat}.

Superposition of FIA^{Sbac} (red) with FIA^{Scat} (blue) as monomer (**a**) and homotrimer (**b**).

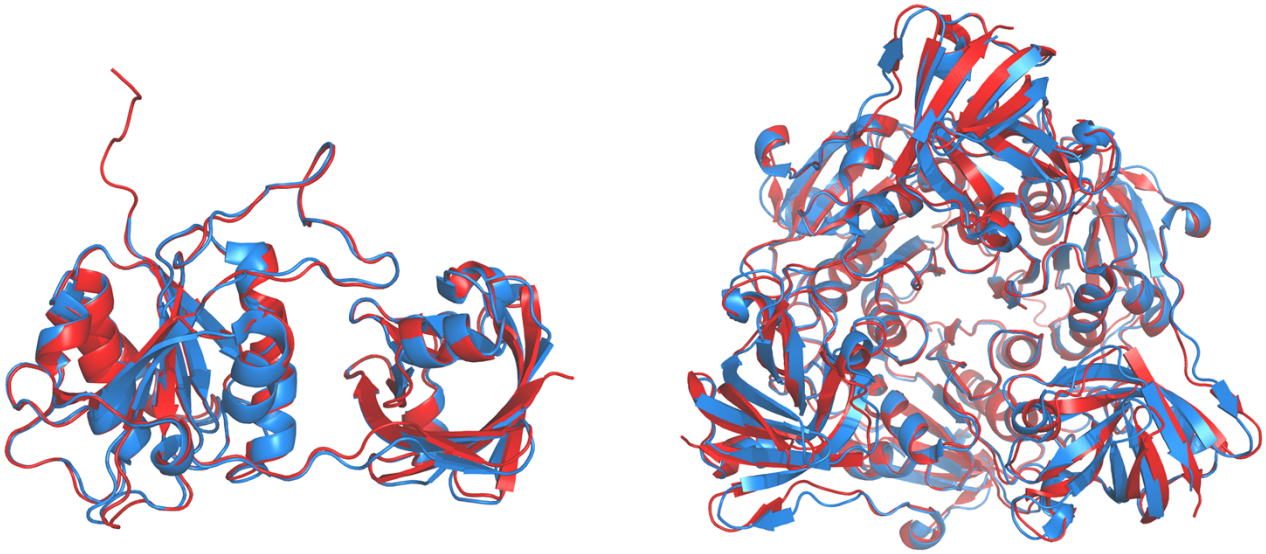

a) **b)**

Fig. S13 The residues in the binding pockets of FIA^{Sbac} and FIA^{Scat}.

Superposition of FIA^{Sbac} (red) with FIA^{Scat} (blue) showing the residues (lines) surrounding SAM (green sticks) within 4 Å. Green sticks: SAM; Red sticks: F50 in FIA^{Sbac}; Blue sticks: W50 in FIA^{Scat}.

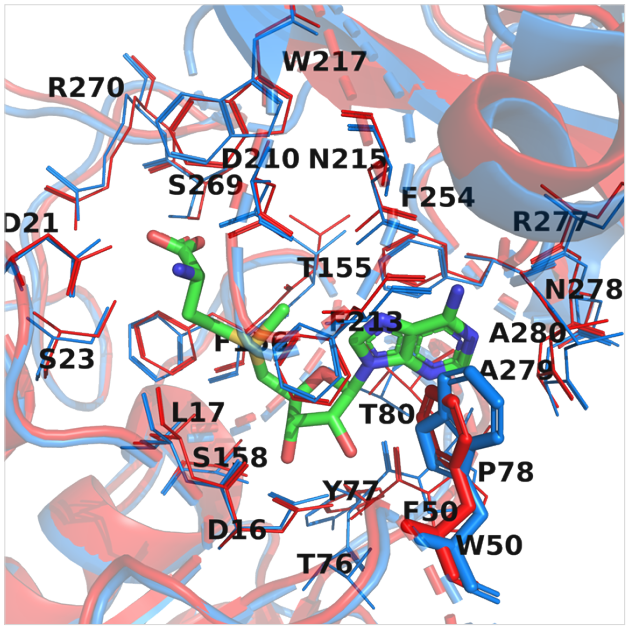

References

1. J. A. Gerlt, J. T. Bouvier, D. B. Davidson, H. J. Imker, B. Sadkhin, D. R. Slater and K. L. Whalen, *Biochimica et Biophysica Acta (BBA) - Proteins and Proteomics*, 2015, **1854**, 1019-1037.
2. R. Zallot, N. Oberg and J. A. Gerlt, *Biochemistry*, 2019, **58**, 4169-4182.
3. R. Saito, M. E. Smoot, K. Ono, J. Ruscheinski, P.-L. Wang, S. Lotia, A. R. Pico, G. D. Bader and T. Ideker, *Nature Methods*, 2012, **9**, 1069-1076.
4. F. Madeira, N. Madhusoodanan, J. Lee, A. Eusebi, A. Niewielska, A. R. N. Tivey, R. Lopez and S. Butcher, *Nucleic Acids Research*, 2024, **52**, W521-W525.
5. K. Tamura, G. Stecher and S. Kumar, *Molecular Biology and Evolution*, 2021, **38**, 3022-3027.
6. J. Jumper, R. Evans, A. Pritzel, T. Green, M. Figurnov, O. Ronneberger, K. Tunyasuvunakool, R. Bates, A. Žídek, A. Potapenko, A. Bridgland, C. Meyer, S. A. A. Kohl, A. J. Ballard, A. Cowie, B. Romera-Paredes, S. Nikolov, R. Jain, J. Adler, T. Back, S. Petersen, D. Reiman, E. Clancy, M. Zielinski, M. Steinegger, M. Pacholska, T. Berghammer, S. Bodenstein, D. Silver, O. Vinyals, A. W. Senior, K. Kavukcuoglu, P. Kohli and D. Hassabis, *Nature*, 2021, **596**, 583-589.
7. N. Wang, J. D. Rudolf, L.-B. Dong, J. Osipiuk, C. Hatzos-Skintges, M. Endres, C.-Y. Chang, G. Babnigg, A. Joachimiak, G. N. Phillips and B. Shen, *Nature Chemical Biology*, 2018, **14**, 730-737.
8. L. Ma, Y. Li, L. Meng, H. Deng, Y. Li, Q. Zhang and A. Diao, *RSC Advances*, 2016, **6**, 27047-27051.
9. P. K. Smith, R. I. Krohn, G. T. Hermanson, A. K. Mallia, F. H. Gartner, M. D. Provenzano, E. K. Fujimoto, N. M. Goeke, B. J. Olson and D. C. Klenk, *Analytical Biochemistry*, 1985, **150**, 76-85.